Check for updates

Received: 25 October 2024 | Revised: 10 January 2025 | Accepted: 21 January 2025

DOI: 10.1002/pc.29625

RESEARCH ARTICLE

Polymer COMPOSITES WILEY

Modeling short fiber reinforced polymer matrix composite materials using material designer

Busra Eyri[1] | **Okan Gul**[1] | **N. Gamze Karsli**[2] | **Taner Yilmaz**[1]

[1]Department of Mechanical Engineering, Kocaeli University, Kocaeli, Turkey

[2]Department of Aviation and Aerospace Engineering, Kocaeli University, Kocaeli, Turkey

Correspondence
Taner Yilmaz, Department of Mechanical Engineering, Kocaeli University, 41380, Kocaeli, Turkey.
Email: taner.yilmaz@kocaeli.edu.tr

Present address
Taner Yilmaz, Department of Mechanical Engineering, Faculty of Engineering, Kocaeli University, Kocaeli, Turkey.

Abstract

In the present era, the importance of simulations pertaining to production is increasing in terms of cost, human resources, and time. As the majority of existing studies on polymer matrix composites are experimental, the development of a modeling approach for these materials will address a significant gap in the existing literature. In order to achieve this objective, the present study investigates the factors influencing the modeling of carbon fiber-reinforced PPS composites produced by the injection molding method with the Ansys Material Designer tool. Composites containing 10% CF by weight were subjected to a tensile test subsequent to production. Subsequently, the tensile strength, elastic modulus, and tensile strain values obtained were then compared with the values were compared with those obtained from the modeled RVEs, with an examination of the various parameters in the Material Designer tool. The requisite parameter values for the optimal model, exhibiting the closest approximation to the experimental results, were derived from the modeled RVEs. The findings of the study indicated that the mean strength of the samples produced was measured at 143.73 MPa. However, when the optimum parameter conditions were met, this value was obtained at 141.48 MPa, with an error of 1.56% in the RVE model. However, this error increased to 18.58% in the elasticity modulus.

Highlights

- The mesh was found to have no significant impact on the outcomes.
- The number of additives in the RVE had a direct effect on the results.
- Changes in the fiber distribution demonstrated comparable outcomes.
- The most crucial parameter for accurately modeling is the RVE size.

KEYWORDS

Ansys, carbon fiber, material designer, modeling, polymer matrix composites, RVE

This is an open access article under the terms of the Creative Commons Attribution-NonCommercial-NoDerivs License, which permits use and distribution in any medium, provided the original work is properly cited, the use is non-commercial and no modifications or adaptations are made.
© 2025 The Author(s). *Polymer Composites* published by Wiley Periodicals LLC on behalf of Society of Plastics Engineers.

1 | INTRODUCTION

Polymers are currently employed in numerous applications on their own, but there is a necessity for reinforcement due to their inadequate mechanical properties. In response to this need, polymer matrix composites (PMC) that are reinforced with long fibers, short fibers (whiskers), or particulates have been developed.[1,2] Polymer matrix composites are employed in a multitude of industrial sectors on a regular basis. Polymer matrix composites play a pivotal role in the development of high-specific strength, corrosion-resistant materials that are simultaneously tougher, lighter, and more functional.[3,4] Short fiber reinforced polymer composites (SFRPCs) represent one of the most widely utilized categories of PMC, offering a straightforward manufacturing process, the ability to produce intricate shapes and a lighter weight compared to numerous traditional materials. Short fiber reinforced polymer composites have been extensively employed in a multitude of engineering fields, including medical components, the chemical industry, automotive applications and aerospace engineering.[5–8] The choice of fibers used depends on the desired mechanical or thermal service conditions, such as higher strength, higher modulus of elasticity, insulation, thermal conductivity or dimensional stability. Until recently, a considerable amount of literature has been published on the use of carbon fibers (CF), glass fibers (GF), boron fibers (BoF), basalt fibers (BF), and so forth.[6,8–10]

The incorporation of carbon fiber into a polymer matrix composite results in a multitude of enhanced material properties, including elevated strength and stiffness, reduced weight, exceptional chemical resistance, electrical conductivity, thermal stability, and superior wear performance.[11–16] In the context of recent advances in composite materials, researchers have examined the effects of CFs on a range of polymer matrices, including polyester resin,[17] polyacrylonitrile (PAN),[18] epoxy resin[19,20] polyamide (PA),[21,22] polycarbonate (PC),[21] polyacrylamide (PAM),[23] polypropylene (PP),[10,14,24] polyisoprene (TPI),[25,26] and acrylonitrile butadiene styrene (ABS).[27] Poly(phenylene sulfide) (PPS) is distinguished among all polymer matrices by a number of exceptional properties, including a tensile strength of approximately 70 MPa, a high melting temperature (*T*m) that enables the use of high service temperatures, high flame resistance, and high dimensional stability. Furthermore, it exhibits high corrosion resistance and requires high temperatures for chemical solubility approximately 200 °C.[16] These remarkable characteristics render it an invaluable matrix for the production of PMC in a multitude of applications. The diverse range of applications for PPS includes aircraft parts, automotive parts, delicate components, such as electric or electronic equipment, impellers, valves, fasteners, and wear rings.[28,29] The extant research on PPS-reinforced short CF has predominantly focused on examining the mechanical, thermomechanical, or tribological properties through experimental means. Furthermore, a concise overview of the extant literature on this topic is provided below. Stoeffler et al. conducted a study on composites comprising a PPS matrix reinforced with recycled CFs sourced from the aerospace industry. The researchers demonstrated that it is feasible to evaluate the mechanical and physical attributes of composites comprising virgin and recycled CF.[30] A further study conducted by Zhang demonstrated that the use of a compatibilizer in CF-reinforced PPS composites enhanced the compatibility between the CF and PPS matrix. Although the compatibilizer had a slight effect on the mechanical properties, the true impact was attributable to the presence of CF.[31] In a subsequent study, the modified PPS was employed once more as a compatibilizer in a CF reinforced PPS composite. The interfacial bonding was found to have been enhanced by an optimal amount of this type of compatibilizer.[32]

As previously stated, the research on PPS and short CF reinforced composites is predominantly experimental in nature. In this regard, experimental studies require a substantial investment of time, resources and equipment. Concurrently, the quality of the samples and the reliability of the tests are contingent upon factors such as the qualifications of the personnel involved and the production conditions.[33] At this juncture, it is of paramount importance to predict the specific properties of materials through the simulation of their behavior. The simulation methods typically employed for composite materials are based on the representation of laminates, which are layered structures. In the representation of short fiber-reinforced composites, where the fiber distribution is random and the orientation depends on numerous factors, numerical models appear to be the optimal approach to describing the behavior of these materials.[5,9] These models facilitate the transformation of heterogeneous materials into constitutively equivalent homogeneous materials. This transformation is achieved through the homogenization method, which represents the heterogeneous properties of the material in the microstructure as a simpler and homogeneous material at the macro scale.[34,35] In order to achieve this, studies are conducted on the smallest repetitive element of the material, which is referred to as the representative volume element (RVE). The RVE contains all phases and additions and represents the material's properties.[36–38]

Commercial software such as Ansys, Abaqus, and Altair has developed tools for the creation of RVE suitable for the composite type with the intention of simplifying stages of the process and increasing their applicability.[34] One such tool is Ansys Material Designer

15480569, 0, Downloaded from https://4spepublications.onlinelibrary.wiley.com/doi/10.1002/pc.29625 by Busra Eyri - Kocaeli Universitesi , Wiley Online Library on [10/02/2025]. See the Terms and Conditions (https://onlinelibrary.wiley.com/terms-and-conditions) on Wiley Online Library for rules of use; OA articles are governed by the applicable Creative Commons License

(MD), the results of which will be presented in this section. In their study, Pai et al.[39] employed the MD software to obtain the RVEs of five distinct types of composites that they had produced. A comparison was conducted between the results of tensile and flexural tests conducted in an experimental setting and those obtained through simulation. The findings revealed a high degree of compatibility between the two approaches. Mali and Paise[34] conducted a comparative analysis of the results obtained from the RVEs of unidirectional, woven, and random composites using MD with various analytical models. The findings of this study indicate that the homogenized properties of composites can be predicted with a degree of accuracy using this tool. In a related study,[37] the importance of the distinction between the RVE model selected in the MD tool and the analytical model employed was emphasized for each elastic property obtained. Yun et al.[40] investigated the impact of aspect ratio on the elastic properties of RVEs generated by MD and compared the findings with those of the Halpin-Tsai model. Sanaka and Sahu[41] conducted a comparative analysis between the experimental outcomes of PU/MXene composite samples produced by injection molding and the corresponding simulations. They observed highly correlated results, with the exception of the Rule of Mixture (ROM) with increasing reinforcement amount, which demonstrated general agreement in the analytical models they utilized. In a separate study,[4] injection-molded samples produced with a HDPE matrix and nanodiamond reinforcement were subjected to experimental testing. The findings revealed that the samples displayed characteristics that were markedly similar to those observed in the MD outcomes. Previous studies have demonstrated that, in addition to a paucity of experimental literature on PPS-CF composites, there is currently no RVE modeling of this type of composite. The present research makes a novel contribution to the field by comparing experimental results with an RVE model of a CF-reinforced PPS composite using MD. The objective of this study is to identify and elucidate the factors that influence the RVE and their effect on the results in comparison to the experimental outcomes.

2 | EXPERIMENTAL METHODOLOGY

2.1 | Composite production

The matrix material employed in this study was PPS, produced by Ticona. It is also known commercially as FORTRON® 1200 L1. The reinforcement material was chopped CF, with a length of 6 mm. The carbon fiber was provided by Dow Aksa. The material properties provided by the suppliers are presented in Table 1. The granulated PPS and CF were subjected to a drying process in a vacuum environment at 80 °C for a period of 12 h prior to injection molding. A twin-screw micro compounder was employed for the melt mixing of the CF-reinforced PPS composites. The melting temperature was set at 310 °C, and the mixing time was 3 min at a screw speed of 100 rpm. The molten material was then injected through the mold at 25 °C under 10 bar pressure. The injection molding process is illustrated in Figure 1. The produced composites were reinforced with 10% by weight of CF.

2.2 | Tensile test

The composites were subjected to tensile testing using an Instron 4411 model tensile test device. The tensile test was conducted in accordance with the ISO-527-2/5A standard, with a speed of 5 mm/min. For each specimen, a

TABLE 1 Properties of matrix and reinforcement materials.

	Poly(phenylene sulphide)	Carbon fiber
Density (ρ)	1.34 g/cm^3	1.76 g/cm^3
Tensile modulus (E)	4 GPa	240 GPa
Tensile strength (σ)	88 MPa	4200 MPa
Glass transition temperature (T_g)	90 °C	–
Melting temperature (T_m)	275 °C	–

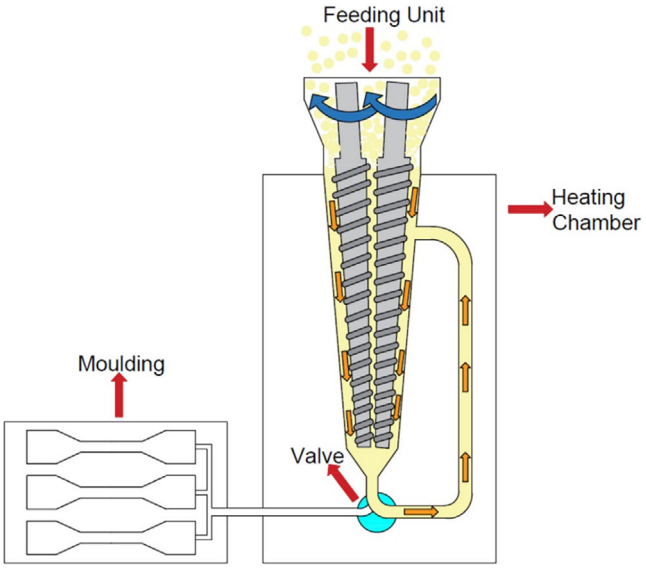


FIGURE 1 The production of tensile test specimens via the injection molding process.

15480569, 0, Downloaded from https://4spepublications.onlinelibrary.wiley.com/doi/10.1002/pc.29625 by Busra Eyri - Kocaeli Üniversitesi , Wiley Online Library on [10/02/2025]. See the Terms and Conditions (https://onlinelibrary.wiley.com/terms-and-conditions) on Wiley Online Library for rules of use; OA articles are governed by the applicable Creative Commons License

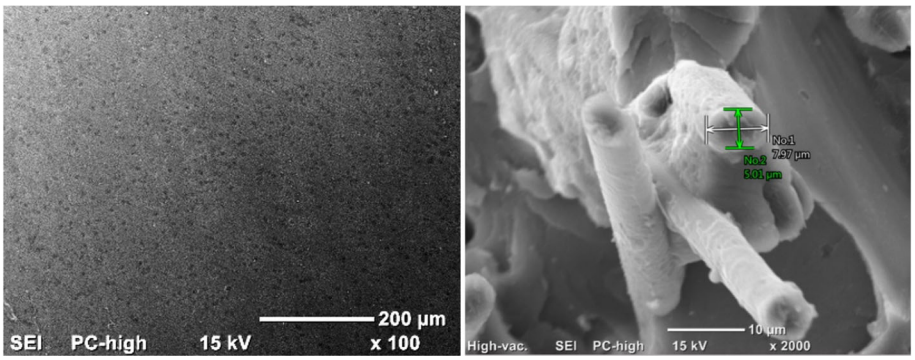


FIGURE 2 SEM micrograph of a material cross-section, with measurements of the diameter of the CFs.

minimum of three tests were conducted, and the mean values of these tests were considered. The tensile test enabled the determination of the tensile strength (σ), tensile modulus (E), and elongation at break (ε) of the specimens.

2.3 | Fiber analysis

It is of the utmost importance to identify the relevant parameters in order to obtain more accurate results that align with the final product. These parameters include the aspect ratio (l/d) value inputted into the Material Designer tool or the orientation of the fibers within the material. In order to achieve this, the diameter of the CF employed as a reinforcing element and its orientation within the material were imaged by means of scanning electron microscopy (SEM). The diameter of the CFs and the SEM micrograph of the material taken from the cross-section perpendicular to the tensile direction are presented in Figure 2. The study was conducted using a Jeol JCM-6000 model SEM. Prior to analysis, the surfaces of the samples were coated with silver in order to ensure conductivity.

The length of the fibers was determined by subjecting the composite samples to combustion in an oven at 600 °C until only the fibers remained. The fibers were then placed on coverslips, followed by the dripping of distilled water and separation of the fibers from each other, in order to obtain a clear image. The average length of the fibers was ascertained by measuring the images obtained using a Nikon SMZ 745T model light microscope (Figure 3).

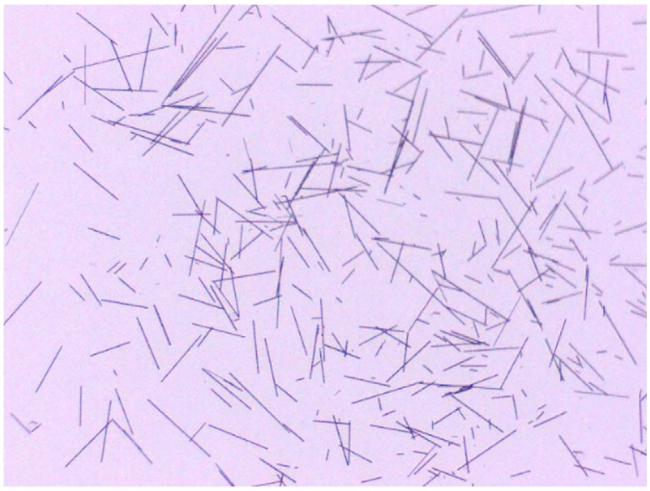


FIGURE 3 The image of the CFs in the composite was obtained using an optical microscope.

3 | NUMERICAL SIMULATION

3.1 | Ansys Granta selector

In instances where materials were not available within Ansys' own library, the Ansys Granta Selector software was employed for the selection of alternative materials. The software provides comprehensive material selection databases, which facilitate more accurate decision-making processes. Granta software was established and developed by Dr. Michael Ashby, a metallurgical and materials engineer. Granta Selector is a comprehensive software program based on the Ashby material selection methodology, which is also named after him and is one of the most widely used methodologies in the world. The software enables the user to identify the most suitable materials for any given application and to export material property data directly.[42] The PPS and CF material data cards obtained from the software were tailored to align with the data in Table 1, which was sourced from the manufacturer. The remaining parameters were maintained at their default settings. Subsequently, the Granta Selector file was linked to the material section of Material Designer, the Ansys RVE modeling tool (Figure 4).

3.2 | Ansys Material Designer

The initial stage of the design and analysis of structures in composite micromechanics is the homogenization

15480569, 0, Downloaded from https://4spepublications.onlinelibrary.wiley.com/doi/10.1002/pc.29625 by Busra Eyri - Kocaeli Universitesi , Wiley Online Library on [10/02/2025]. See the Terms and Conditions (https://onlinelibrary.wiley.com/terms-and-conditions) on Wiley Online Library for rules of use; OA articles are governed by the applicable Creative Commons License

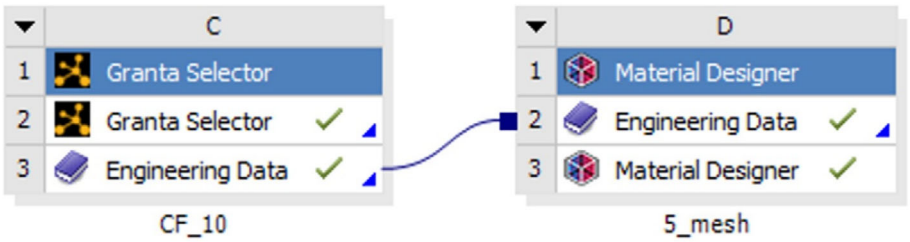


FIGURE 4 Linking the Granta selector file to the material designer tool.

process. The elastic properties of a heterogeneous material at the micro level can be determined by homogenization, which allows the stiffness of the material to be quantified. This enables an examination of the material's behavior at the macro level.[43] A number of models have been developed with the objective of determining these elastic constants. Material Designer is a modeling tool designed for the determination of material properties through the generation of an RVE (representative volume element) based on the Mori-Tanaka model. The Mori-Tanaka model is used to ascertain the distribution of the reinforcement phase within the matrix material and to determine the contribution of this distribution to the macroscopic elastic properties. The Mori-Tanaka process can be summarized as follows[35]:

1. The identification of matrix and reinforcement phases,
2. Calculation of the Eshelby tensor which is employed to ascertain the behavior of the reinforcement phase within the matrix,
3. The determination of strain in the reinforcement phase,
4. Calculation of the effective strain,
5. Expression of the deformation of the reinforcement,
6. Expression of matrix strain,
7. Determination of the macroscopic elastic modulus of the composite material.

In the context of Material Designer, the following assumptions are made with regard to short-fiber reinforced composites:[44]

- The matrix material exhibits isotropic linear elastic behavior.
- In contrast, the fiber material is either isotropic or transversely isotropic (in one direction) and exhibits linear elastic behavior.
- Fibers are cylinders of finite length, which necessitates the utilization of the Eshelby tensor for ellipsoidal inclusions.
- The length and diameter of all fibers are identical.
- The interfacial bond between the fibers and the matrix material is optimal.
- The RVE is characterized by a periodicity.

The following options for the design of short fiber reinforced composite materials in the Material Designer tool are modifiable in accordance with the specifications outlined.

Fiber Weight Fraction: In light of the fact that the fiber weight fraction is 10% in the present study, this value is designated as the input.

Aspect Ratio: In the context of composite materials, the aspect ratio is defined as the ratio of the length to the diameter of the reinforcing element. In order to obtain this value, the fiber analysis presented in section 2.3 was conducted, resulting in an input value of 25.

Repeat Count: An increase in this number will result in an expansion of the RVE, which in turn will lead to an increase in the number of reinforcements included in it.[44] The importance of ensuring statistical homogeneity of the RVE has been emphasized in previous studies, as this is crucial for more accurate representation. Furthermore, it is of the utmost importance to select a RVE of sufficient size to ensure the independence of boundary conditions.[5] In order to ascertain the critical size, another parameter that will be considered in this study is the repeat count.

Orientation Tensor: The orientation tensor was devised to quantify the degree of alignment between the fibers in the composite and the corresponding direction. If it is assumed that the direction unit vector for the RVE with N fibers is d^1, d^2, ..., d^N, then the tensor can be expressed as follows:

$$a_{i,j} = \sum_{k=1}^{N} d_i^{(k)} d_j^{(k)} \quad (1)$$

The Material Designer tool is utilized to generate a RVE in which the principal axes of the orientation tensor are aligned with the spherical coordinate system. Subsequently, three values, a11, a22, and a33, must be input. These values indicate the degree of alignment between the fibers and the corresponding direction of alignment. It is of great importance to ascertain the orientation of the fibers within the internal structure during the

15480569, 0, Downloaded from https://4spepublications.onlinelibrary.wiley.com/doi/10.1002/pc.29625 by Busra Eyri - Kocaeli Universitesi , Wiley Online Library on [10/02/2025]. See the Terms and Conditions (https://onlinelibrary.wiley.com/terms-and-conditions) on Wiley Online Library for rules of use; OA articles are governed by the applicable Creative Commons License

production process. The orientation of fibers orientation is of great importance, as it affects the behavior of the material. In the context of injection molding, the mold walls exert a considerable influence on the manner in which the material flows into the mold. In the material that freezes instantaneously upon entering the mold, the fibers are randomly distributed. The effect of this region is so minimal that it can be disregarded. The regions of the flowing material in close contact with the mold are subjected to shear stresses, which serve to influence the orientation of the fibers. While the fibers tend to orientate in a direction parallel to the mold flow direction (MFD), in the core region, which is relatively further away from the mold, this orientation is perpendicular to the MFD. Given that the level of shear stress is diminished in this area, these regions are designated the skin, shell, and core, respectively. The thickness of the regions is contingent upon a number of manufacturing parameters. In this study, the fiber orientation was set at 70% in the direction of the MFD, in accordance with the literature.[3,45–47] The resulting fiber orientation matrix for the RVE and its representation are presented in Figure 5.

$$a_{i,j} = \begin{bmatrix} a_{11} & 0 & 0 \\ 0 & a_{22} & 0 \\ 0 & 0 & a_{33} \end{bmatrix}$$

$$a_{i,j} = \begin{bmatrix} 0{,}7 & 0 & 0 \\ 0 & 0{,}15 & 0 \\ 0 & 0 & 0{,}15 \end{bmatrix}$$

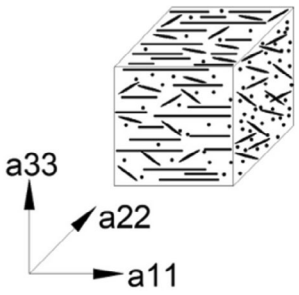


FIGURE 5 The orientation matrix and representation of oriented fibers on the RVE.

Seed: The MD tool employs an algorithm, designated as Sequential Addition with Orientation Optimization, for the distribution of fibers in the composite. The algorithm is responsible for the random and non-overlapping distribution of fibers in accordance with the specified fiber orientation.[48] In this context, the term 'seed' refers to the number of RVE algorithms that are reconstructed each time with this algorithm. In the present study, a series of fiber distributions were generated and their influence on the final material was assessed.

4 | RESULTS AND DISCUSSION

4.1 | Tensile test

A total of three samples were produced, comprising both pure PPS samples and composite samples labeled PPS_CF. Figure 6A illustrates the tensile curves of the PPS_CF. In order to gain a deeper insight into the reinforcement of the CF within the matrix, a comparison of the values obtained from the tensile test results is presented in Figure 6B. As demonstrated in the accompanying figure, the tensile strength and modulus values of the unreinforced PPS are enhanced by the addition of CF. This enhancement in mechanical properties with fiber reinforcement is an anticipated outcome and is elucidated by the "rule of mixtures" in extant literature.[10] Additionally, the effect of interfacial bonding on the mechanical strength of composite materials is a well-established phenomenon, as evidenced by previous research.[49,50] Consequently, the enhanced load-carrying capacity observed in the manufactured samples can be ascribed to the exceptional mechanical properties of CF and the establishment of a exceedingly effective interface between the PPS matrix and the CF. Moreover, the

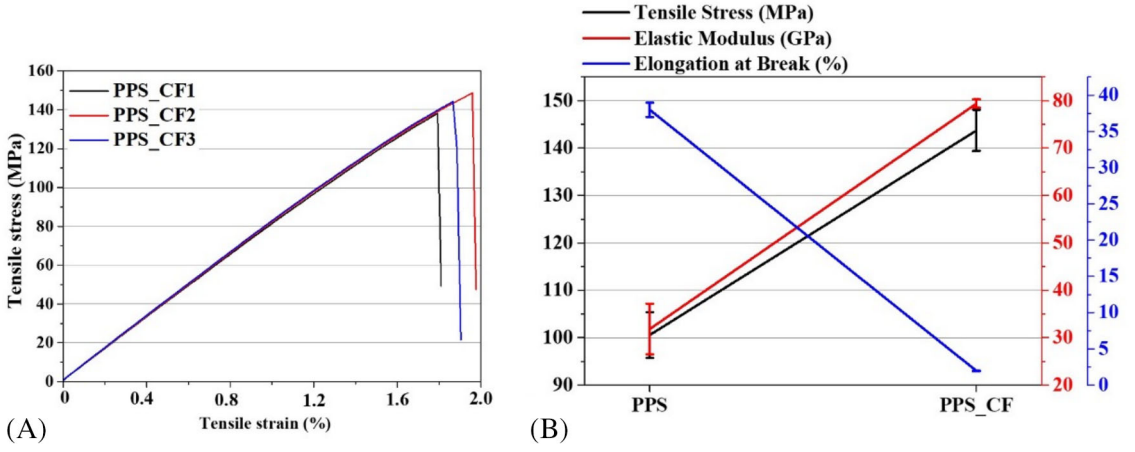


FIGURE 6 (A) Tensile test curves of the composite specimens, (B) Comparison of tensile test results of pure PPS and composites.

15480569, 0, Downloaded from https://4spepublications.onlinelibrary.wiley.com/doi/10.1002/pc.29625 by Busra Eyri - Kocaeli Universitesi , Wiley Online Library on [10/02/2025]. See the Terms and Conditions (https://onlinelibrary.wiley.com/terms-and-conditions) on Wiley Online Library for rules of use; OA articles are governed by the applicable Creative Commons License

uniform and agglomeration-free distribution of the CF can be attributed to the consistent pattern observed in the curves. This effect can also be observed in the SEM micrographs provided in Section 2.

Table 2 presents the tensile strength, modulus, and elongation at break values of the composites with 10% CF-reinforced PPS matrix produced in the study. It is evident that the values observed are consistent with those documented in existing literature, thereby demonstrating a notable degree of enhancement in the tested samples in comparison to the reference matrix material. The average strength value for PPS material reinforced with 10% CF, as reported by Karslı et al.,[51] was 147.87 MPa. However, Kızıl et al.[16] measured this value to be 146.0 MPa. Moreover, the modulus and elongation values presented in the aforementioned studies are consistent with those observed in the current study. The observed reduction in elongation at break can be explained by the failure mechanism described in the literature.[10] According to this mechanism, when subjected to tensile stress, microcracks initiate at the fiber ends due to heightened stress concentration at these points. These cracks then propagate along the fiber direction, disseminating throughout the matrix until reaching a critical level at which point the composite undergoes final fracture. This outcome demonstrates that fracture is closely related to the number of fiber ends. Another reason for the decrease in elongation at break can be attributed to the decrease in the mobility of polymer chains with the addition of fibers. The incorporation of a rigid reinforcement material into a polymer matrix can result in enhanced interfacial interaction between the reinforcement material and the matrix material, leading to the homogeneous distribution of the reinforcement material within the polymer matrix. This distribution occurs between the polymer chains, thereby reducing their mobility.[52] This, in turn, reduces the polymer's elastic deformation ability when an external load is applied.

Table 3 presents the mean values and standard deviations derived from the samples. These values are consistent with the trends observed in the curves illustrated in Figure 6-a and fall within the acceptable range of deviations.

TABLE 2 The values obtained from the tensile test results of the composite specimens.

	PPS_CF1	PPS_CF2	PPS_CF3
σ_y (MPa)	138.14	148.73	144.32
E (GPa)	78.25	79.53	80.42
ε (%)	1.87	2.02	1.95

The following sections will present a comparison between the data obtained from the material models created with the Material Designer tool and the aforementioned mean values.

4.2 | Mesh Independence

An investigation into the effects of the mesh parameter on the material properties using the Material Designer tool revealed no significant impact. This was determined through an analysis of three different meshes for 5, 10, and 20, with all other parameters (seed, repeat count, etc.) held constant. The mesh sizes indicated herein are defined as the maximum element size. Table 4 illustrates the impact of varying mesh values on the stress corresponding to each strain value. The slight fluctuations observed in the stress values suggest that the issue is not dependent on the mesh. Given the proximity of the results, the mash value of 10 was selected for all simulations.

4.3 | Repeat count

This section presents the findings of a parameter investigation into the influence of the RVE size of the modeled material on the analysis. The incorporation of a sufficient number of reinforcements within the RVE, coupled with a satisfactory number of interface connections between these elements and the matrix, enables the convergence of the material properties. The study employed a RVE with varying repeat counts, spanning 2, 3, 4, and 5, and the resulting graphs are presented in Figure 7.

TABLE 3 Mean values and standard deviations of the data obtained from tensile tests.

	Average
σ_y (MPa)	143.73 ± 4.35
E (GPa)	79.40 ± 0.89
ε (%)	1.95 ± 0.064

TABLE 4 Impact of varying mesh values on the stress corresponding to each strain value.

Mesh size Strain (mm/mm)	5	10	20
0.010	88.98 MPa	88.97 MPa	88.98 MPa
0.015	120.78 MPa	120.77 MPa	120.77 MPa
0.020	143.13 MPa	143.11 MPa	143.12 MPa

15480569, 0, Downloaded from https://4spepublications.onlinelibrary.wiley.com/doi/10.1002/pc.29625 by Busra Eyri - Kocaeli Üniversitesi , Wiley Online Library on [10/02/2025]. See the Terms and Conditions (https://onlinelibrary.wiley.com/terms-and-conditions) on Wiley Online Library for rules of use; OA articles are governed by the applicable Creative Commons License

As illustrated in the graph, the model demonstrates a progressive convergence with the experimental result as the repeat count number increases. It has been demonstrated in previous studies that the values obtained from comparatively larger RVEs are more consistent with the results of experiments.[5,53] Nevertheless, an alternative study that considers the size of the RVE has demonstrated that the values remain relatively constant beyond a certain size.[41] As illustrated in the graph, the deviation values become so insignificant after a certain number that they can be considered negligible. Consequently, an accurate evaluation of material characteristics may not be feasible if the RVE volume is insufficient to meet the minimum requirements for accurate approximation.[54] In the present study, the optimal repeat count was determined to be 5 for the composite comprising PPS and CF.

4.4 | Seed number

A more precise estimation of material characteristics may be achieved through the repeated simulation of fiber distributions. As each distribution represents a different production probability, the possible distributions of the material will affect its properties.[3,36] Accordingly, RVEs comprising three distinct random distributions were generated via the algorithm outlined in Section 3. The tensile curves presented in Figure 8A are compared with the curve obtained from the experimental test. As illustrated in the figure, the simulation and experiment are in accordance with one another, with the discrepancy in fiber distribution resulting in an inconsequential alteration to the curves.

The mean column in Table 5 provides the mean and standard deviation values of the tensile strength and modulus values for the three distinct RVEs. It was demonstrated that the variance within the RVEs obtained from the algorithm remained relatively minimal. The values in the error column indicate the discrepancy between the data obtained from the RVEs and the average value of the experimental data. Accordingly, while there is a high level of agreement between the tensile strength values and the experimental data, there is a discrepancy of 18.58% between the modulus values and the experimental data. A similar study demonstrated that as the reinforcement ratio in the composite material increases, the error rate in the modulus also rises. The highest error rate was observed at a reinforcement ratio of 10% by volume.[41] However, this value is lower than the modulus error rate obtained from RVEs produced with the same tool in the existing literature.[39] Accordingly, the value of 14,720 for the seed was deemed to be acceptable. Accordingly, the optimal RVE has been generated by the MD tool for CF-reinforced PPS composite material. The selected values for

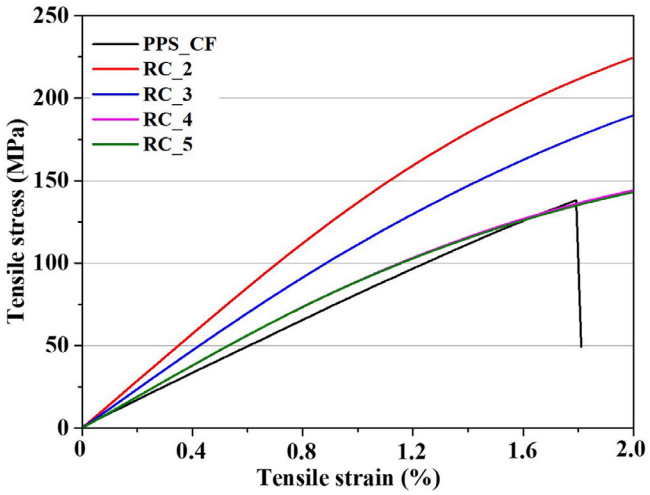
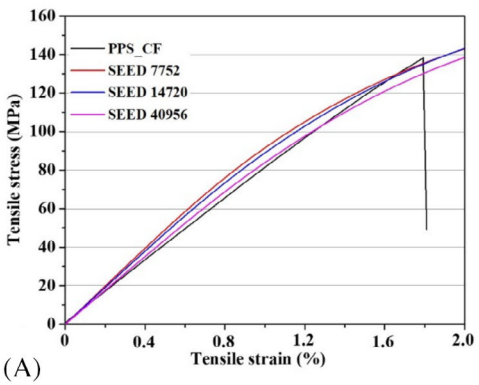


FIGURE 7 The tensile test curves for RVE with varying repeat counts.

TABLE 5 The tensile test results for the RVEs, together with a comparison with the corresponding experimental values.

	Average	% Error
σ_y (MPa)	141.48 ± 2.12	1.56
E (GPa)	94.15 ± 4.53	18.58



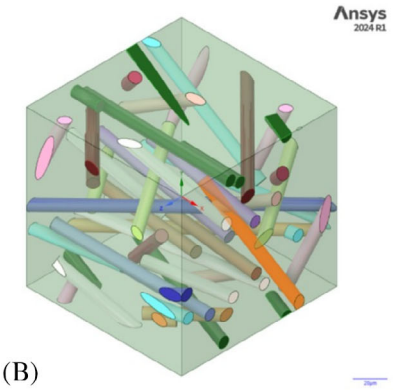


FIGURE 8 (A) The tensile test curves for RVE samples generated by different fiber distributions, (B) Optimum RVE obtained from MD.

15480569, 0, Downloaded from https://4spepublications.onlinelibrary.wiley.com/doi/10.1002/pc.29625 by Busra Eyri - Kocaeli Üniversitesi , Wiley Online Library on [10/02/2025]. See the Terms and Conditions (https://onlinelibrary.wiley.com/terms-and-conditions) on Wiley Online Library for rules of use; OA articles are governed by the applicable Creative Commons License

this RVE are as follows: the aspect ratio is 25, the maximum element size (mesh) is 10, the repeat count is 5 and the seed number is 14720. As no fracture occurred in the MD tool, the strain was limited to 0.2%. The image of the RVE obtained from the ANSYS Material Designer tool for the optimum data is presented in Figure 8B.

5 | CONCLUSION

In this study, the material properties obtained by Material Designer, a material modeling tool produced by Ansys commercial software, were compared with the experimental results. The effect of varying the parameters within the MD tool on the material properties has been subjected to analysis. Consequently, an attempt was made to ascertain the factors that should be taken into account in order to obtain the most optimal material model. It was determined that the most significant effect in the modeling process was due to the repeat count, and the curve that exhibited the closest resemblance to the experimental result was obtained with a repetition number of 5. The aspect ratio for the produced composite material was taken as 25 as a result of the measurements, which was effective in the convergence of the final curve to the experimental one. The fiber orientation was accepted as 70%, and it was determined that this was a correct assumption according to the optimum result obtained. The number of meshes had no significant effect on the model. The various RVEs obtained from the fiber distribution algorithm were within or close to the range of the data obtained from the experimental test. Therefore, although the seed number taken as the basis is 14,720, selecting other seed numbers would also remain within the solution range and be considered correct. In general, the tensile strength values obtained from the MD tool are in close agreement with the actual material properties, with a mean value of 141.48 ± 2.12 MPa and a modulus value of 94.15 ± 4.53. The discrepancies between the simulation and experimental results can be attributed to the presence of voids, agglomeration, interface imperfections, or experimental errors in the material, given that the MD tool assumes a perfect manufacturing process and composite interface. Therefore, from the perspective of the material production process, material modeling with MD may offer a more efficient option for the industry, given the potential loss of time, capital, and manpower.

ACKNOWLEDGMENTS

This study was conducted in collaboration with Numesys, the distributor and partner of Ansys in Turkey. The authors would like to express their gratitude to Mr. Ahmet Okudan and Mr. Bilal Şen for their invaluable contributions to this study.

CONFLICT OF INTEREST STATEMENT

The authors declare no conflicts of interest.

DATA AVAILABILITY STATEMENT

The datasets generated and supporting the findings of this article are obtainable from the corresponding author upon reasonable request.

ORCID

Busra Eyri https://orcid.org/0000-0002-1775-3688
Taner Yilmaz https://orcid.org/0000-0002-1520-6744

REFERENCES

1. Boopathy G, Balaji G, Bhoominathan R, Bejaxhin ABH, Ramanan N. Enhancing mechanical characteristics and cost-efficiency of composite materials through hybridization and nanoparticle incorporation. In: Sumesh M, Tavares RS, Vettivel SC, Oliveira MO, eds. *2nd International Conference on Smart Sustainable Materials and Technologies (ICSSMT 2023). ICSSMT 2023. Advances in Science, Technology & Innovation*. Springer; 2024. doi:10.1007/978-3-031-49826-8_11
2. Prabakaran T, Ramkumar K, Bovas Herbert Bejaxhin A, et al. Development of eco-natural fibre composite and its strength determination using tribological and optimized experimental outcomes with SEM views. *J Inst Eng India Ser D*. 2024. doi:10.1007/s40033-024-00647-2
3. Sharma A, Munde Y, Kushvaha V. Representative volume element based micromechanical modelling of rod shaped glass filled epoxy composites. *SN Appl Sci*. 2021;3(2):1. doi:10.1007/s42452-021-04261-9
4. Sahu SK, Rama Sreekanth PS. Multiscale RVE modeling for assessing effective elastic modulus of HDPE based polymer matrix nanocomposite reinforced with nanodiamond. *Int J Interact Des Manuf*. 2022;18:6371. doi:10.1007/s12008-022-01080-z
5. Kari S, Berger H, Gabbert U. Numerical evaluation of effective material properties of randomly distributed short cylindrical fibre composites. *Comput Mater Sci*. 2007;39(1):198-204. doi:10.1016/j.commatsci.2006.02.024
6. Mortazavian S, Fatemi A. Fatigue behavior and modeling of short fiber reinforced polymer composites: a literature review. *Int J Fatigue*. 2015;70:297-321. doi:10.1016/j.ijfatigue.2014.10.005
7. Isaincu A, Dan M, Ungureanu V, Marsavina L. Numerical investigation on the influence of fiber orientation mapping procedure to the mechanical response of short-fiber reinforced composites using Moldflow, Digimat and Ansys software. *Mater Today Proc*. 2021;45:4304-4309. doi:10.1016/J.MATPR.2020.12.792
8. Jiang L, Zhou Y, Jin F. Design of short fiber-reinforced thermoplastic composites: a review. *Polym Compos*. 2022;43(8):4835-4847. doi:10.1002/pc.26817
9. Kulkarni A, Aswini N, Dandekar CR, Makhe S. Modeling of short fiber reinforced injection moulded composite. *IOP Conf*

15480569, 0, Downloaded from https://4spepublications.onlinelibrary.wiley.com/doi/10.1002/pc.29625 by Busra Eyri - Kocaeli Üniversitesi , Wiley Online Library on [10/02/2025]. See the Terms and Conditions (https://onlinelibrary.wiley.com/terms-and-conditions) on Wiley Online Library for rules of use; OA articles are governed by the applicable Creative Commons License

Ser Mater Sci Eng. 2012;40:012025. doi:10.1088/1757-899X/40/1/012025

10. Karsli NG, Aytac A, Deniz V. Effects of initial fiber length and fiber length distribution on the properties of carbon-fiber-reinforced-polypropylene composites. *J Reinf Plast Compos*. 2012;31(15):1053-1060. doi:10.1177/0731684412452678
11. Yu K, Shi Q, Dunn ML, Wang T, Qi HJ. Carbon fiber reinforced thermoset composite with near 100% recyclability. *Adv Funct Mater*. 2016;26(33):6098-6106. doi:10.1002/adfm.201602056
12. Kada D, Koubaa A, Tabak G, Migneault S, Garnier B, Boudenne A. Tensile properties, thermal conductivity, and thermal stability of short carbon fiber reinforced polypropylene composites. *Polym Compos*. 2018;39:E664. doi:10.1002/pc.24093
13. Gao X, Huang Y, He X, et al. Mechanically enhanced electrical conductivity of polydimethylsiloxane-based composites by a hot embossing process. *Polym Basel*. 2019;11(1):56. doi:10.3390/polym11010056
14. Rezaei F, Yunus R, Ibrahim NA. Effect of fiber length on thermomechanical properties of short carbon fiber reinforced polypropylene composites. *Mater Des*. 2009;30(2):260-263. doi:10.1016/j.matdes.2008.05.005
15. Chen Z, An T, Lu K, et al. Mechanical property and thermal stability of short carbon fiber reinforced polysulfonamide composites. *Polym Compos*. 2024;45(6):5009-5016. doi:10.1002/pc.28105
16. Kizil A, Dincer U, Yilmaz S, Gul O, Karsli NG, Yilmaz T. Investigation of the effect of zeolite, bentonite, and basalt fiber as natural reinforcing materials on the material properties of PPS and CF-reinforced PPS. *Polym Eng Sci*. 2023;63(4):1314. doi:10.1002/pen.26285
17. Zhang J, Wang X, Fu X. High mechanic enhancement of chopped carbon fiber reinforced-low-density unsaturated polyester resin composite at low preparation temperature with facile polymerization. *Materials*. 2021;14(15):4273. doi:10.3390/ma14154273
18. Maheshwari PH, Gupta C, Mathur RB. Role of fiber length and pore former on the porous network of carbon paper electrode and its performance in PEMFC. *Fuel Cells*. 2014;14(4):566-573. doi:10.1002/fuce.201300290
19. El Sawi I, Olivier PA, Demont P, Bougherara H. Processing and electrical characterization of a unidirectional CFRP composite filled with double walled carbon nanotubes. *Compos Sci Technol*. 2012;73:19-26. doi:10.1016/j.compscitech.2012.08.016
20. Ozsoy N, Ozsoy M, Mimaroglu A. Mechanical properties of chopped carbon fiber reinforced epoxy composites. *Acta Phys Pol A*. 2016;130(1):297-299.
21. Clingerman ML, King JA, Schulz KH, Meyers JD. Evaluation of electrical conductivity models for conductive polymer composites. *J Appl Polym Sci*. 2002;83(6):1341-1356. doi:10.1002/app.10014
22. Akasheh F, Aglan H. Fracture toughness enhancement of carbon fiber–reinforced polymer composites utilizing additive manufacturing fabrication. *J Elastomers Plast*. 2019;51(7–8):698. doi:10.1177/0095244318817867
23. Zeng C, Gu Y, Xie Y, et al. Eco-friendly preparation of carbon-bonded carbon fiber based on glucose-polyacrylamide hydrogel derived carbon as binder. *Nanomaterials*. 2023;13(6):1045. doi:10.3390/nano13061045
24. Altay L, Seki Y, Sever K, et al. Effect of compatibilizer on morphology, thermal and mechanical properties of recycled carbon fiber reinforced polypropylene composites. *Acta Phys Pol A*. 2018;134(1):196-199. doi:10.12693/APhysPolA.134.196
25. Guo J, Wang Z, Tong L, Lv H, Liang W. Shape memory and thermo-mechanical properties of shape memory polymer/carbon fiber composites. *Compos Part A Appl Sci Manuf*. 2015;76:162-171. doi:10.1016/j.compositesa.2015.05.026
26. Wang Z, Liu J, Guo J, Sun X, Xu L. The study of thermal, mechanical and shape memory properties of chopped carbon fiber-reinforced TPI shape memory polymer composites. *Polym Basel*. 2017;9(11):594. doi:10.3390/polym9110594
27. Tekinalp HL, Kunc V, Velez-Garcia GM, et al. Highly oriented carbon fiber–polymer composites via additive manufacturing. *Compos Sci Technol*. 2014;105:144-150. doi:10.1016/j.compscitech.2014.10.009
28. Chen G, Mohanty AK, Misra M. Progress in research and applications of polyphenylene sulfide blends and composites with carbons. *Compos B Eng*. 2020;209:108553. doi:10.1016/j.compositesb.2020.108553
29. Aslan C, Karsli NG. Investigation of the synergetic effect of hybrid fillers of hexagonal boron nitride, graphene nanoplatelets and short basalt fibers for improved properties of polyphenylene sulfide composites. *Polym Bull*. 2024;81(6):4969-4992. doi:10.1007/s00289-023-04940-0
30. Stoeffler K, Andjelic S, Legros N, Roberge J, Schougaard SB. Polyphenylene sulfide (PPS) composites reinforced with recycled carbon fiber. *Compos Sci Technol*. 2013;84:65-71. doi:10.1016/J.COMPSCITECH.2013.05.005
31. Zhang K, Zhang G, Liu B, Wang X, Long S, Yang J. Effect of aminated polyphenylene sulfide on the mechanical properties of short carbon fiber reinforced polyphenylene sulfide composites. *Compos Sci Technol*. 2014;98:57-63. doi:10.1016/J.COMPSCITECH.2014.04.020
32. Ren H, Xu D, Yan G, et al. Effect of carboxylic polyphenylene sulfide on the micromechanical properties of polyphenylene sulfide/carbon fiber composites. *Compos Sci Technol*. 2017;146:65-72. doi:10.1016/J.COMPSCITECH.2017.03.021
33. Zachariah SA, Shenoy BS, Pai KD. Comprehensive analysis of in-plane tensile characteristics of thin carbon/ aramid hybrid composites using experimental and RVE-based numerical study. *Compos Struct*. 2021;271:114160. doi:10.1016/j.compstruct.2021.114160
34. Mali R, Pise U. Modeling elastic properties of biocomposites using various analytical models and ansys material designer. *Mater Today Proc*. 2023;72:1372. doi:10.1016/j.matpr.2022.09.334
35. Gupta A, Hasanov S, Fidan I, Zhang Z. Homogenized modeling approach for effective property prediction of 3D-printed short fibers reinforced polymer matrix composite material. *Int J Adv Manuf Technol*. 2022;118(11–12):4161-4178. doi:10.1007/s00170-021-08230-9
36. Berger H, Kari S, Gabbert U, Ramos RR, Castillero JB, Díaz RG. Evaluation of effective material properties of randomly distributed short cylindrical fiber composites using a numerical homogenization technique. *J Mech Mater Struct*. 2007;2(8):1561. doi:10.2140/jomms.2007.2.1561

15480569, 0, Downloaded from https://4spepublications.onlinelibrary.wiley.com/doi/10.1002/pc.29625 by Busra Eyri - Kocaeli Universitesi , Wiley Online Library on [10/02/2025]. See the Terms and Conditions (https://onlinelibrary.wiley.com/terms-and-conditions) on Wiley Online Library for rules of use; OA articles are governed by the applicable Creative Commons License

37. Alhijazi M, Safaei B, Zeeshan Q, Arman S, Asmael M. Prediction of elastic properties of thermoplastic composites with natural fibers. *J Text Inst*. 2023;114(10):1488-1496. doi:10.1080/00405000.2022.2131352
38. Jayaraman P, Pai A, Rodriguez-Millan M, Shenoy BS, Chethan KN, Hegde S. Exploring acoustic properties of banana fiber composites with elastomeric filler through a computational approach. *Mater Res Express*. 2024;11(1):015508. doi:10.1088/2053-1591/ad1e0b
39. Pai A, Suri R, Bhave AK, Verma P, P NH. Puck's criterion for the tensile response of composite laminates: a numerical approach. *Adv Eng Softw*. 2023;175:103364. doi:10.1016/j.advengsoft.2022.103364
40. Yun DH, Yun JH, Jeon YJ, Kang MS. Analysis of elastic properties according to the aspect ratio of UHMWPE fibers added to PP/UHMWPE composites. *Appl Sci*. 2022;12(22):11429. doi:10.3390/app122211429
41. Sanaka R, Sahu SK. FEM based RVE modeling for estimating axial modulus of polyurethane composite reinforced with MXene. *Int J Interact Des Manuf*. 2023;18:3259. doi:10.1007/s12008-023-01485-4
42. Ansys Granta Selector, Materials Selection Software. https://www.ansys.com/products/materials/granta-selector
43. Bin Rayhan S, Rahman M. Modeling elastic properties of unidirectional composite materials using Ansys material designer. *Procedia Struct Integr*. 2020;28:1892-1900. doi:10.1016/j.prostr.2020.11.012
44. Material Designer User's Guide. Ansys® Material Designer, Release 2023 R2, Help System, Material Designer User's Guide. ANSYS, Inc.
45. Akay M, Barkley D. Fibre orientation and mechanical behaviour in reinforced thermoplastic injection mouldings. *J Mater Sci*. 1991;26(10):2731-2742. doi:10.1007/BF02387744
46. Horst JJ, Spoormaker JL. Fatigue fracture mechanisms and fractography of short-glassfibre-reinforced polyamide 6. *J Mater Sci*. 1997;32(14):3641. doi:10.1023/A:1018634530869
47. Bernasconi A, Davoli P, Basile A, Filippi A. Effect of fibre orientation on the fatigue behaviour of a short glass fibre reinforced polyamide-6. *Int J Fatigue*. 2007;29(2):199-208. doi:10.1016/j.ijfatigue.2006.04.001
48. Ansys I. *Material Designer User's Guide*. ANSYS Inc; 2023. http://www.ansys.com
49. Yang L, Thomason JL. Interface strength in glass fibre–polypropylene measured using the fibre pull-out and microbond methods. *Compos Part A Appl Sci Manuf*. 2010;41(9):1077-1083. doi:10.1016/j.compositesa.2009.10.005
50. Wang R, Cao Z, Hao L, Jiao W, Yang F, Liu W. Healing carbon fiber/polymer Interface by resistive heating. *Polym Polym Compos*. 2014;22(3):337-340. doi:10.1177/096739111402200317
51. Karsli NG, Gul O, Yilmaz T. Investigation of the synergistic effect of addition the hybrid carbon fiber, graphene nanoplatelet and matrix modifier to poly(phenylene sulphide) on physical properties. *Fibers Polym*. 2022;23(4):1059-1067. doi:10.1007/s12221-022-4215-z
52. Sahin AE, Karsli NG, Sinmazcelik T. Comparison of the mechanical, Thermomechanical,Thermal, and morphological properties of pumice and calcium carbonate-filled poly(phenylenesulfide) composites. *Polym Compos*. 2016;37(11):3160. doi:10.1002/pc.23513
53. Valavala PK, Odegard GM, Aifantis EC. Influence of representative volume element size on predicted elastic properties of polymer materials. *Model Simul Mater Sci Eng*. 2009;17(4):45004. doi:10.1088/09650393/17/4/045004
54. Yim SO, Lee WJ, Cho DH, Park IM. Finite element analysis of compressive behavior of hybrid short fiber/particle/mg metal matrix composites using RVE model. *Met Mater Int*. 2015;21(2):408-414. doi:10.1007/s12540-015-4306-0

How to cite this article: Eyri B, Gul O, Karsli NG, Yilmaz T. Modeling short fiber reinforced polymer matrix composite materials using material designer. *Polym Compos*. 2025;1-11. doi:10.1002/pc.29625

15480569, 0, Downloaded from https://4spepublications.onlinelibrary.wiley.com/doi/10.1002/pc.29625 by Bursa Eyri - Kocaeli Üniversitesi , Wiley Online Library on [10/02/2025]. See the Terms and Conditions (https://onlinelibrary.wiley.com/terms-and-conditions) on Wiley Online Library for rules of use; OA articles are governed by the applicable Creative Commons License